

Evaluation of In-plane Flux Distribution in 3Phase 100kVA Transformer Core

Dina Maizana

Abstract – These papers describe the result of measurement and evaluate the behaviours of in-plane flux distribution on 100kVA 3phase distribution transformer assembled with the combination of 60°-45° T-joint. Methodology that is used in this investigation is measurement of flux distributions in transformer core by using no load test and arrays of search coil in Cold Roll Grain Oriented (CRGO) material of transformer core lamination. The measurement involves the fundamental and third harmonics component of the easy and hard direction of flux density at each location measurement. The instantaneous flux flow through the core within one magnetising cycle is analysed with displaced by 120° in time. The locus of the localised flux distribution throughout the magnetising cycle is illustrated the rotational flux produced in the T-joint region of the three-phase three limbs transformer core. The localized flux density at the outer of combination of 60°-45° T-joint is 1.4T and rises to be 1.68T at the inner edges of right yoke passes over to the butt joint of middle limb when the transformer core energized at flux density 1.5 T 50Hz. At the same place the high third harmonic of peak in-plane flux is 0.23T. The transfer of flux between lamination takes place until a point is reached where the material in the region butt joint of yoke lamination, which is directly above the butt joint and the flux higher but did not reaches saturation.

Keywords: Transformer core, in-plane flux, magnetic behavior, locus

I. Introduction

A Transformer is designed to transfer electrical energy from AC voltage to another with high efficiency. This performance characteristic is achieved through a combination of the special dimensions of the transformer and the materials that are used in its fabrication [1]. Although the power loss of large transformers may be less than 0.5% of the total power output, significant savings might still be possible by improved core and joint design. Circulating and rotational fluxes make large contributions to the total power loss in three-phase transformer cores, and it is thought that they might be minimized by correct design [2-4]. The extra losses are due to factors such as flux deviating from the rolling direction of magnetization and flux harmonics in localised regions of the core [5]. Flux density that is flow through the transformer core is not uniform. The maximum flux density is found in the centre limb of the transformer core [6].

The flux distribution in individual laminations can be measured using arrays of search coils [7]. The instantaneous flux distribution variation throughout a

cycle can be calculated with the help of a suitable computer program.

The major efficiency of transformer can be reached if the transformer is designed to operate near or below the knee of the magnetic performance curve for the steel core materials. This practice avoids the core operating to the saturation region of magnetic performance curve which would cause the no load loss and magnetizing currents to increase sharply [1].

Norman P. Goss developed grain orientation processing in the 1930s in the USA after finding that suitably applied cold rolling and heat treatment regimes led to the selective growth of grains having their easy directions of magnetization in the strip rolling direction [8]. The Grain oriented, or Goss textured material has a strong [001] (110) texture of grains along its rolling directions giving it very anisotropic magnetic properties with lowest loss and highest permeability when magnetized along that direction [9]. Today only grain – oriented steel is used by cold rolling the steel sheets. The magnetic domains in the steel sheets will tend to be oriented in the rolling direction. Cold rolled silicon steel is supplied by the marker to guarantee the maximum total loss, at a specified value of maximum flux density, usually 1.5T [10].

The objective of this investigation is to know the in-plane flux distribution of the transformer core built from electrical steel that call M5 with 3% silicon iron assembled with the combination of 60°- 45° T-joint core by using arrays of search coils.

II. Experiment Apparatus and Measuring Technique

The main apparatus consist of a model cores three-phase 100kVA transformer assembled with three limbs core with the combination of 60°- 45° T-joint core of three phase core. The core has 550 mm x 580 mm with the limbs and yokes 100 mm wide as shown in Fig. 1 and Fig. 2 and assembled from 0.3 mm thick laminations of Cold Roll Grain Oriented (CRGO).

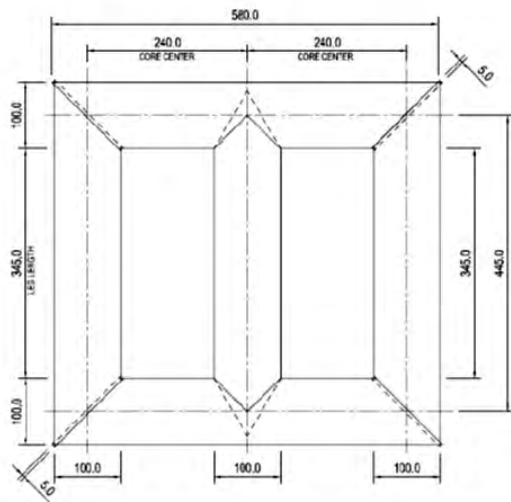


Fig. 1. Dimension (mm) of 100kVA transformer model

The localized flux density distribution in individual laminations is measured using search coils. And the test circuit for localised flux distribution measurement as shown in Fig. 3 and 4. The samples are drilled with an aid of drilling machine. It is constructed from 0.15 mm diameter wire treaded through 0.8 mm diameter holes 10 mm a part as shown in Fig. 5. The search coil induced voltages are analysed to find the magnitude and plane coil induced voltage of flux density by using power analyzer as shown in Fig. 4. Each measuring position suitable coils are wound to measure the easy and hard direction flux density.

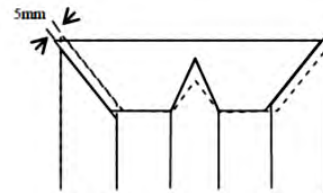


Fig. 2. Transformer core type the combination of 60°- 45° T-joint core

A transformer core which is magnetised by a sinusoidal voltage generates a flux density waveform containing only odd harmonic. Flux distribution in the Cold Rolled Grain Oriented (CRGO) is measured by using an array of search coils to get the satisfactory result. In this investigation an array of single turn search coil is employed to measure in-plane (longitudinal and transverse) of flux density in the lamination within the transformer core.

The in-plane flux density variations at T-joint configuration use the search coil. Because the flux tends to deviate out of the longitudinal direction in some region, small 10mm search coils are used to measure localized longitudinal and transverse flux component. The locations are chosen to cover the areas where the flux is more likely to vary direction so as to find distribution of the flux behavior as shown in Fig. 6.

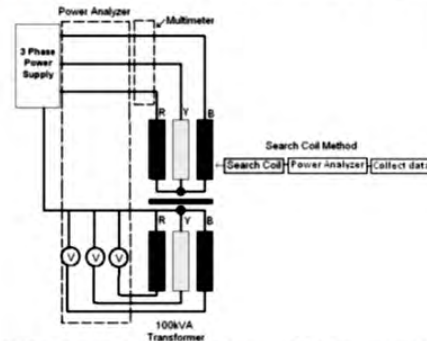


Fig. 3. The diagram of the methods that used to measure the localised flux density

In the corner configuration the 101mm overall search coils were placed parallel to the end of the lamination so that a detailed study of the overall flux density along the lamination could be made is shown in fig. 7.



Fig. 4. Test circuit for localised flux distribution measurement

The testing process is done by using the No-Load Test Frame. The No-Load Test Frame consisting of three windings for each three phase core are designed in order not only to avoid introducing stress to the laminations but also to keep the magnetism exactly constant in all limbs of the cores. Each winding only extends along 85% on each limb in order to enable the stagger length of the three phase core to be varied. An extra softwood base 200mm high is used to raise the overall height of the core, in order to minimize the effect of the stray flux on the localized measurements.

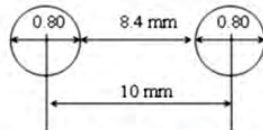


Fig. 5. Dimensions [mm] of the holes drilled in the specimen

Installation search coil takes quite a long time in completing this step which every hole needs to be inserted with search coil. Search coil is the enamel copper coated 0.1mm diameter wire. Each set of test point (4 holes) consists of easy and hard direction where the holes of easy and hard direction will be inserted search coil and the leads are twisted together. All the holes at testing point need to be repeated the same method of inserting and twisting the leads. The Fig. 8 has shown complete wiring on lamination.

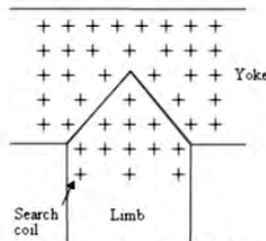


Fig. 6. Location of orthogonal search coils in the three phase core

After the search coils are wound and the leads twisted together, the holes are filled with polyurethane varnish to give added insulation protection. The search coil leads, which are twisted to prevent any spurious pick up, are stuck to the lamination by a polyurethane varnish. The leads from all the search coils are taken to a junction box placed in the core to prevent any interference from the core or magnetising windings.



Fig. 7. Location of overall search coils in the corner region of the three phase core

All the search coils when fixed into position were tested for continuity, insulation, strength and polarity. It was necessary to check the polarity of these coils, in order to determine the direction of the flux enclosed by each search coil.



Fig. 8. Complete wiring on lamination for search coils method.

A U-shaped core was employed energised by an a.c. voltage supply as indicated in figure 09. The U-shaped core had a single winding with a large number of turns to limit the a.c. current. One channel of oscilloscope connected to power supply and other channel of oscilloscope connected to search coil. The U-core placed on a lamination above the search coil to be tested in such away that the flux path was perpendicular to the plane of the search coil. The emf induced in the search coil due to the U-core. The magnetisation flux was displayed on the same oscilloscope, and its polarity was compared with a reference signal. If the two signals are in phase as in figure 10 then the output of the search coil signal has the same polarity as the reference voltage.

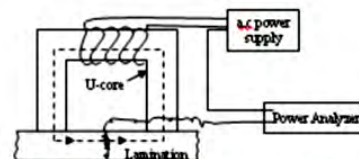


Fig. 9. A U-shaped core was employed energised by an A.C. voltage supply, showing the position of the C core relative to search coil for longitudinal and transverse search coil

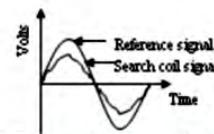


Fig. 10. The output of the search coil signal

Fig. 11 shows a schematic diagram of the apparatus used for measuring the magnitude and phase of the harmonics in the emfs induced in the search coils. The induced voltages are routed via the selector box was amplified by an interface and selected channel is related to channel power analyzer. At the beginning of this measurement the system is checked by ensuring that the

The testing process is done by using the No-Load Test Frame. The No-Load Test Frame consisting of three windings for each three phase core are designed in order not only to avoid introducing stress to the laminations but also to keep the magnetism exactly constant in all limbs of the cores. Each winding only extends along 85% on each limb in order to enable the stagger length of the three phase core to be varied. An extra softwood base 200mm high is used to raise the overall height of the core, in order to minimize the effect of the stray flux on the localized measurements.

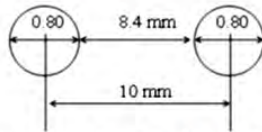


Fig. 5. Dimensions [mm] of the holes drilled in the specimen

Installation search coil takes quite a long time in completing this step which every hole needs to be inserted with search coil. Search coil is the enamel copper coated 0.1mm diameter wire. Each set of test point (4 holes) consists of easy and hard direction where the holes of easy and hard direction will be inserted search coil and the leads are twisted together. All the holes at testing point need to be repeated the same method of inserting and twisting the leads. The Fig. 8 has shown complete wiring on lamination.

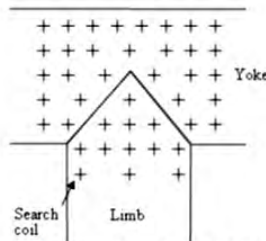


Fig. 6. Location of orthogonal search coils in the three phase core

After the search coils are wound and the leads twisted together, the holes are filled with polyurethane varnish to give added insulation protection. The search coil leads, which are twisted to prevent any spurious pick up, are stuck to the lamination by a polyurethane varnish. The leads from all the search coils are taken to a junction box placed in the core to prevent any interference from the core or magnetising windings.



Fig. 7. Location of overall search coils in the corner region of the three phase core

All the search coils when fixed into position were tested for continuity, insulation, strength and polarity. It was necessary to check the polarity of these coils, in order to determine the direction of the flux enclosed by each search coil.



Fig. 8. Complete wiring on lamination for search coils method.

A U-shaped core was employed energised by an a.c. voltage supply as indicated in figure 09. The U-shaped core had a single winding with a large number of turns to limit the a.c. current. One channel of oscilloscope connected to power supply and other channel of oscilloscope connected to search coil. The U-core placed on a lamination above the search coil to be tested in such away that the flux path was perpendicular to the plane of the search coil. The emf induced in the search coil due to the U-core. The magnetisation flux was displayed on the same oscilloscope, and its polarity was compared with a reference signal. If the two signals are in phase as in figure 10 then the output of the search coil signal has the same polarity as the reference voltage.

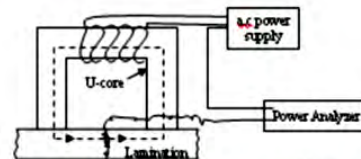


Fig. 9. A U-shaped core was employed energised by an A.C. voltage supply, showing the position of the C core relative to search coil for longitudinal and transverse search coil

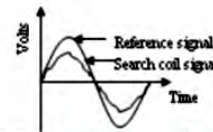


Fig. 10. The output of the search coil signal

Fig. 11 shows a schematic diagram of the apparatus used for measuring the magnitude and phase of the harmonics in the emfs induced in the search coils. The induced voltages are routed via the selector box was amplified by an interface and selected channel is related to channel power analyzer. At the beginning of this measurement the system is checked by ensuring that the

emf induced in a twisted wire with the same length as a search coil is zero to ensure that no pick up is present.

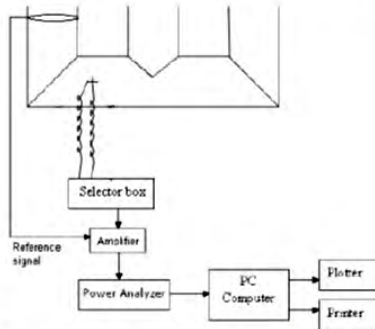


Fig. 11. Schematic diagram of the apparatus used to measure the magnitudes of localised flux density

The converted voltage data from the search coil is passed power analyzer and then to a computer which is used to calculate the magnitude and direction of the harmonic components of the localised flux density throughout the magnetising cycle at each coil site. The magnitude of localised flux density of any individual harmonic component could be measured to within $\pm 1\%$. The magnitude and corresponding phase angle, of orthogonal search coil induced voltage, e_x and e_y and their phase angle, ϕ_x and ϕ_y is displayed on the computer monitor or printed out.

The instantaneous magnitude and direction of the localised flux density can be calculated from the voltage induced in the search coils. Consider a point in the lamination where the average induced emfs is detected by a pair of orthogonal search coil SC_x and SC_y . The corresponding flux density in these coils must be of

the form:

$$b_{nx}(t) = \frac{-e_{nx}}{4NfA} \cos_{nx} n(\omega t + \theta_{nx}) \quad (1)$$

and

$$b_{ny}(t) = \frac{-e_{ny}}{4NfA} \cos_{ny} n(\omega t + \theta_{ny}) \quad (2)$$

Where

e_{nx} = induced e.m.f. of SC_x

e_{ny} = induced e.m.f. of SC_y

θ_{nx} = phase difference of the nth harmonic component of $e_x(t)$ with respect to the fixed reference

θ_{ny} = phase difference of the nth harmonic component of $e_y(t)$ with respect to the fixed reference

N = number of turns of search coil = 1T
 A = cross sectional area of the magnetic material enclosed by search coil

$$= \frac{3}{1000} \times \frac{10}{1000} \times 1 \text{ [m}^2\text{]}$$

f = fundamental frequency = 50Hz

n = harmonic number 1, 3.

The losses are different due to the effect of the change in peak flux on the core loss [11,12]. To show how different relative phase angles of the third harmonic flux influence losses it can be seen in figure 12. The resultant flux densities plotted against time at different relative phase angles of the third harmonic flux in figure 12 (a), if the fundamental and third harmonic are in phase, the resultant has peak value at A; while, if the third harmonic is 90° lagging, the peak value (Fig.12 (b)) is at B.

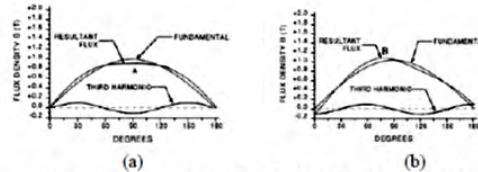


Fig. 12. The resultant flux densities plotted against time at (a) fundamental and the third harmonic flux in phase, (b) the third harmonic is 90° lagging.

III. Result and Discussion

III.1. Distribution of fundamental component of localised flux density

The fluxes flowing in the limbs of the three phase core are displaced by 120° in time, it is important to analyse the instantaneous flux flow through the core within one magnetising cycle. In this section the localised flux density is presented as a vector representing the instantaneous magnitude and direction of the flux density at selected instants in time within a cycle.

Fig. 13 shows the flux distribution in three cores at the instant when $\omega t=0^\circ$, $\omega t=60^\circ$ and $\omega t=120^\circ$. Fig. 13(a) shows the flux distribution in three cores at the instant when the total fluxes in the (R)-phase outer limb is maximum and both the yellow (Y) and Blue (B)-phase limbs carry half of their maximum flux. The flux distribution in the T-joint region is presented on a large scale in Fig. 14 (a). At this instant, in left yoke all of flux is directed towards the middle limb and the next flux in other direction. Most of the flux in all laminations of the core remains in the longitudinal direction except in part of the T-joint region and middle limb lamination.

The flux mainly stays in rolling direction because of the high anisotropy of the steel. The magnitude drops at the butt joints in T-joint are approached as flux diverts to

adjacent laminations above and below to avoid the high reluctance air gap. The magnitude is high at the points where there are butt joints in adjacent laminations.

The instantaneous magnitude and direction of flux at the $\omega t=60^\circ$ is shown in Fig. 13(b) and 14(b) on a large scale at this instant the total flux in the (Y)-phase middle limb reaches its maximum and both (R) and (B)-phases outer limbs carry half their maximum flux. At this instant, in yoke more flux tends to move toward the middle limb on the inner region of the yoke lamination but the outside it remains along the rolling direction. By considering the variation of the flux through the magnetizing cycle, it is found that the flux is purely alternating in all areas of yoke. It can be seen from flux direction of right yoke, where the fluxes flow from right to left. Whereas at instant in time when $\omega t = 0$, flux direction of right yoke is from left to right. For flux direction of left yoke can change with comparing at time instant when $\omega t = 120^\circ$, that can be seen in Fig. 14(c).

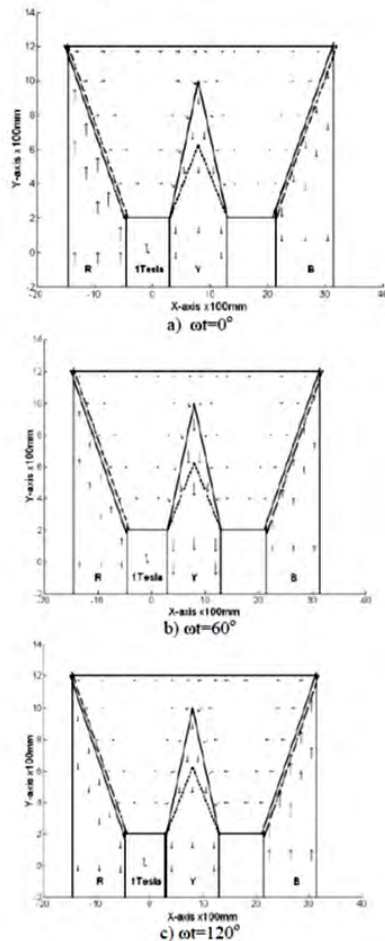


Fig. 13. Distribution of the fundamental component of localised in-plane flux density in the combination of 60° - 45° T-joint core of three

phase core at different instant in time when (a) $\omega t=0^\circ$, (b) $\omega t=60^\circ$ and (c) $\omega t=120^\circ$

Since the yokes carry only half the maximum value of the total flux the majority of the flux from the (R) and (B)-phases outer limbs is carried through the inner half of butt-joint of middle limb in the core and the fundamental component of flux tends to remain in the rolling direction throughout the T-joints.

Core material situated above all butt-joints in alternate layers of lamination is subjected to an increase in flux density while the magnitude of flux density at the butt-joint is. The fact that flux density increases in a material situated above a butt joint and decreases towards the end of each lamination indicates flux transfer in this region.

The transfer of flux between lamination takes place until a point is reached where the material in the region butt joint of yoke lamination, which is directly above the butt joint and the flux higher but did not reaches saturation. The fact that the material has flux higher increases the path reluctance so the horizontal path now has lower reluctance than that offered by the small air gap between laminations so forcing the remaining flux in path R and path B of yoke lamination to across the region of butt joint.

The instantaneous magnitude and direction of flux at the $\omega t=120^\circ$ is shown in Fig. 13(c) and 14(c) on a large scale. At this instant the total flux in the (B)-phase outer limb reaches its maximum and both the (R) and (Y) phase limbs carry half their maximum flux. At this instant, in right yoke more flux tends to move toward the middle limb on the inner region of the yoke lamination but the outside it remains along the rolling direction.

The magnitude of the flux density varies considerably across the least excited limb. Flux entering the T-joint region from the left yoke more deviation turns at the core combination of 60° - 45° T-joint cores of three phase core lamination.

The instantaneous fundamental component of flux density distribution shows that the flux follows the longitudinal direction of the strip in the yoke and limb until it is very close to the overlap length at the outer corner joint where it tends to rotate into the overlap region itself. This is because in the overlap region close to the region above the butt-joint the material is highest flux.

The instantaneous flux distribution of the fundamental component shows that the increasing width of the yoke by increased overlap area length the combination of 60° - 45° T-joint cores causes a higher deviation of the flux from the longitudinal direction as shown in Fig. 14(c). The flux leaving the T-joint through the yoke into the (B)-phase outer limb deviates from the longitudinal direction of the strip in the combination of 60° - 45° T-joint core due to the higher level of anisotropy of 3% silicon iron material which allows more flux to deviate away from the longitudinal direction when the overlap area is increased.

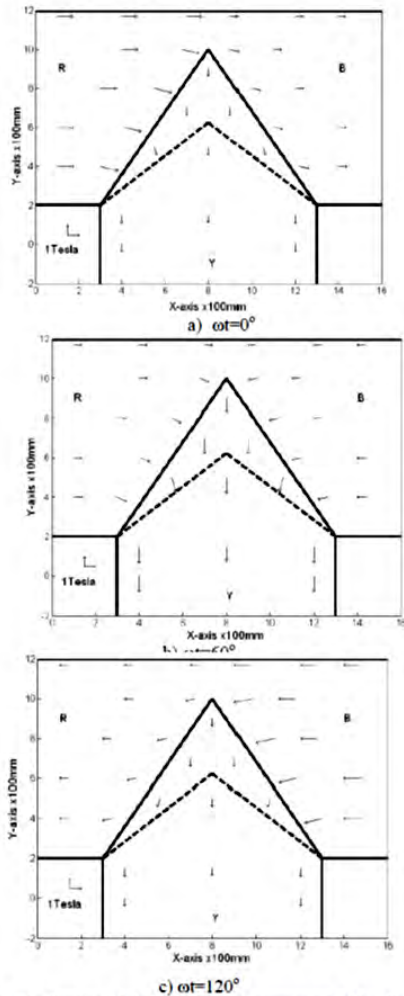


Fig. 14. Distribution of the fundamental component of localised in-plane flux density in the combination of 60°-45° T-joint core of three phase core at different instant in time when (a) $\omega t=0^\circ$, (b) $\omega t=60^\circ$ and (c) $\omega t=120^\circ$

III.2. Distribution of third harmonic component of localised flux density

The magnitude and direction of the third harmonic flux in the plane of laminations of cores at the instant when (a) $\omega t_3 = 0^\circ$, (b) $\omega t_3 = 60^\circ$ and (c) $\omega t_3 = 120^\circ$ at a core flux density of 1.5T is shown in figure 15. From Fig. 15(a) that the third harmonics component magnitude of flux is about thirteen of the corresponding fundamental of flux. Local generation of the third harmonic component of flux occurs in the T-joint regions. Third harmonic flux is evident in the upper region of the butt joint between middle limb and left yoke lamination. At

Fig. 15 (b) $\omega t_3 = 60^\circ$ this instant the flux at the yoke lamination has decreased. They are wide deviations away from the longitudinal direction throughout the T-joint area. In Fig. 15 (c) shows third harmonic flux is evident in the right yoke lamination. Inside the T-joint of left yoke and the middle limb, the flux has decreased.

III.3. Locus of the localised flux density

The rotational flux produced in the T-joint region of the three-phase three limbs transformer core are due to a combined effect of alternating and rotating fields. This rotational flux illustrates the locus of the localised flux distribution throughout the magnetising cycle.

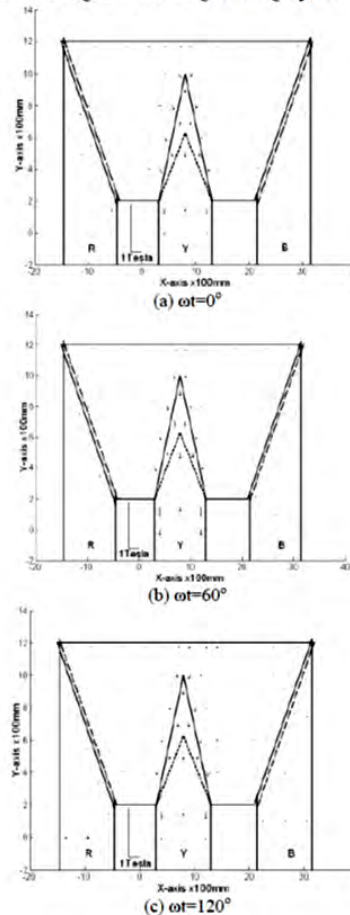


Fig. 15. Distribution of the third harmonic component of localised in-plane flux density in the combination of 60°-45° T-joint core of three phase core at different instant in time when (a) $\omega t_3=0^\circ$, (b) $\omega t_3=60^\circ$ and (c) $\omega t_3=120^\circ$

The rotational flux of the 1st and 3rd harmonic component of flux density in the combination of 60°-45° T-joint cores of three phase core from the location of search coils has been studied and compared. Repeatability tests on other laminations confirmed the

rotational flux distributions such that all measuring locations, even the small fifth harmonic loci, were reproduced to within $\pm 1\%$.

The loci of the fundamental component (50Hz) of flux density the combination of 60° - 45° T-joint core of three phase core at a core flux density of the 1.5T are shown in figure 16. At each point the magnitude and direction variation of the flux density throughout the cycle is shown. The diagrams show that in the core rotational flux does occur in the above of butt joint of yoke area and it is indicated by elliptical pattern. There is little deviation (in-plane of the lamination) apart from where rotational flux is occurring. The high of anisotropy in the silicon iron material causes no rotational flux at other area in the T-joint as indicated by the straight line pattern. Where the locus is a straight line, the flux is alternating.

The third harmonic is another important component of flux density. Figure 16(b) shows the loci of the third harmonic component of flux density in the combination of 60° - 45° T-joint core of three phase core at core flux density of 1.5T. The third distribution of the harmonic component was similar to that of the fundamental component in the core although the magnitude is lower.

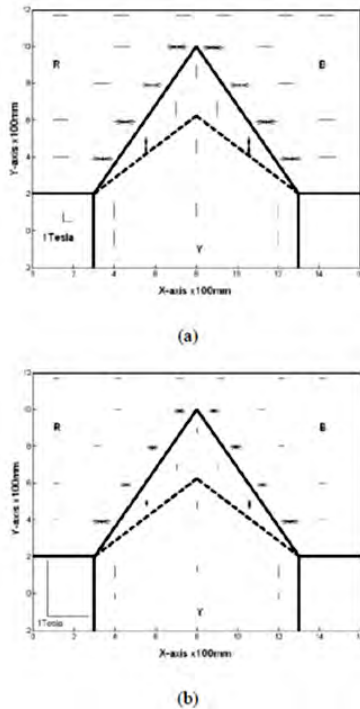


Fig. 16. Locus of the (a) fundamental and (b) third harmonic component of localised flux density in the combination of 60° - 45° T-joint core of three phase core at flux density of the 1.5T, 50Hz

III.4. Distribution of the in-plane flux density

The localised variation in the magnitude of peak flux density measured in the T-joint of core assembled with

the combination of 60° - 45° T-joint core of three phase core at core flux density of 1.5T is shown in Fig. 17(a). There is a wide variation in flux density across the centre of the T-joint.

The localised variation in the magnitude of the third harmonic component of peak flux density measured in the combination of 60° - 45° T-joint core of three phase core at core flux density of 1.5T is shown in Fig. 17(b). Most of the high third harmonic flux occurs in the T-joint region. There is a wide variation in flux density across the centre of the T-joint.

The localised flux density will increase from the outer to the inner edge of the combination of 60° - 45° T-joint. The localised flux density at the outer of combination of 60° - 45° T-joint is 1.4T and rises to be 1.68T at the inner edges of right yoke passes over to the butt joint of middle limb when the transformer core energized 1.5 T 50Hz. The high third harmonic of peak in-plane flux occurs at the inner edge of right yoke passes over to the butt-joint of middle limb is 0.23T

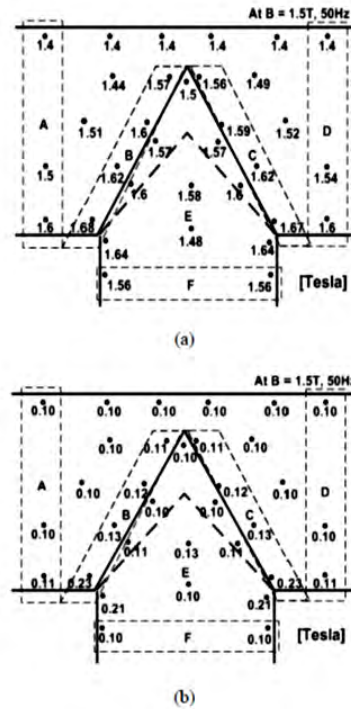


Fig. 17. Local variations in the Tesla of the (a) fundamental and (b) third harmonic peak in-plane flux density of the lamination in the combination of 60° - 45° T-joint core of three phase core at 1.5T, 50Hz

IV. Conclusion

From the result of this investigation is found that the variation of the flux through the magnetizing cycle shows

that the flux is purely alternating in all areas of yoke. The high of anisotropy in the silicon iron material causes no rotational flux at other area in the T-joint as indicated by the straight line pattern. Where the locus is a straight line, the flux is alternating. The localised flux density will increase from the outer to the inner edge of the combination of 60°- 45° T-joint. The localised flux density at the outer of combination of 60°- 45° T-joint is 1.4T and rises to be 1.68T at the inner edges of right yoke passes over to the butt joint of middle limb when the transformer core energized at flux density 1.5 T 50Hz. At the same place the high third harmonic of peak in-plane flux is 0.23T. The third distribution of the harmonic component was similar to that of the fundamental component in the core although the magnitude is lower.

The difference in flux densities in various parts of the core causes temperature gradients especially near the joint producing high power loss due to the combination. But this design still efficient because the flux flows in the transformer core lamination did not reach saturation.

Acknowledgements

This work was supported by FRGS 2010 research grant.

References

- [1] Ahmed M.A. Haidar, S. Taib, I. Daut & S. Uthman., Evaluation of Transformer Magnetizing Core Loss, *Journal of Applied Sciences*, 6 (12), 2006, pp.2579-2585
- [2] Mirzaie M., Yazdani-Asrami M., Sadati S.B. and Shayegani Akmal A., Impacts of Non- Sinusoidal Load Currents on Distribution Transformer Losses-Part I: Theoretical Aspects and Finite Element Based Simulation, *International Review of Electrical Engineering (IREE)*, Vol.6, n.5, October 2011. pp2207- 2214.
- [3] Mirzaie M., Yazdani-Asrami M., Sadati S.B. and Shayegani Akmal A., Impacts of Non- Sinusoidal Load Currents on Distribution Transformer Losses-Part II: Standard Aspects and Experimental Measurement, *International Review of Electrical Engineering (IREE)*, Vol.6, n.5, October 2011. pp2215- 2220.
- [4] Anthony J. Moses and Bleddyn Thomas, Problems in the Design of Power Transformers, *IEEE Trans on Mag*, vol. Mag-10, no. 2, 1974, pp 148-150.
- [5] Basak, A. and Moses, A.J., Harmonic losses in a Three Phase Transformer Core, *IEEE Trans. On Mag.*, 14(5), 1978, 990-992
- [6] Dina, M.M. Ahmad¹, I. Daut², S.Taib³, Flux Simulation on 100kVA Three-Phase Transformer Core, *International Review on Modeling and Simulation (I.R.E.M.O.S.)*, Vol.3, N.3, June 2010. ISSN 1974-9821
- [7] Daut, I. *Investigation of Flux and Loss Distribution in Transformer Cores Assembled From Amorphous Powercore Material*, PhD Thesis University of Wales, (1992), pp. 63-80
- [8] Philip Beckley., *Electrical steels for rotating machines, the institution of Electrical Engineers*, London, and United Kingdom, 2002.

- [9] Moses A.J. & Leicht J., Characterising Soft Magnetic Materials used in Electrical Power Applications, <http://www.iee.org/OnComms/sector/power/PN-Article.cfm>.
- [10] Stigant, S Austen and A.C. Franklin, *The JSP Transformer Book*, Newnes-Butter Worths London, 1980, pp. 13-15
- [11] Rupanagunta, P., Hsu, J.S., Weldon, W.F., Determination of Iron Core losses Under Influence of Third-Harmonic Flux Component, *IEEE Trans. On Mag.*, 27(2), 1991, pp768-777
- [12] Sadati, S. B., Yazdani-Asrami M. and Taghipour M., Effects of Harmonic Current Content and Ambient Temperature on Load Ability and Life Time of Distribution Transformer, *International Review of Electrical Engineering (IREE)*, Vol.5, n.4, August 2010, pp1444-1451

Authors' information

¹School of Electrical System Engineering, University Malaysia Perlis (UniMAP) , Jl.1, Taman Seberang Jaya pasar 3, postcode 02000, Kuala Perlis, Email: dina@unimap.edu.my and dina_maizana@yahoo.com



Dina Maizana received her Eng. from University of North Sumatera, Indonesia in 1991. MSc in Electrical Conversion from Institute of Bandung Technology, Indonesia in 1995 and PhD in Electrical System at University of Malaysia Perlis (UniMAP) in 2011. Her research interest is Transformer design. She has authored and co-authored more than 89 technical papers in the national, international journal and conferences.